PCCP

ROYAL SOCIETY OF CHEMISTRY

PAPER

View Article Online
View Journal | View Issue

Cite this: *Phys. Chem. Chem. Phys.*, 2024, **26**, 24894

Exploring h-BN as a hydrogen conductor and depository†

Ekaterina V. Sukhanova, *[a] Anton M. Manakhov, [b] Andrey Kovalskii,[b] Abdulaziz S. Al-Qasim[c] and Zakhar I. Popov *[ad]

Received 20th June 2024,
Accepted 5th September 2024

DOI: 10.1039/d4cp02466d

rsc.li/pccp

The use of hexagonal boron nitride (h-BN) as a material for hydrogen storage is attributed to its ability to accommodate atomic and molecular hydrogen. However, the low diffusion barrier of molecular hydrogen within the h-BN structure does not fully explain the long-term stability of hydrogen bubbles observed in experimental work [L. He, H. Wang, L. Chen, X. Wang, H. Xie, C. Jiang, C. Li, K. Elibol, J. Meyer, K. Watanabe, T. Taniguchi, Z. Wu, W. Wang, Z. Ni, X. Miao, C. Zhang, D. Zhang, H. Wang and X. Xie, *Nat. Commun.*, 2019, **10**, 2815, **https://doi.org/10.1038/s41467-019-10660-9**]. Another unresolved inquiry is the method by which hydrogen infiltrates the h-BN layer in a perpendicular direction. In this study, we conducted a comprehensive examination of several aspects that can impact the permeation of hydrogen in the h-BN structure. We employed DFT within the rPBE (DFT-D3(0)) functional to suggest a process for the penetration of atomic hydrogen through the h-BN sheet along the normal direction by sequential hydrogen passivation.

Introduction

An increase in global energy consumption necessitates the development of alternative fuels, in particular hydrogen fuel, because hydrogen is environmentally friendly and the most abundant element in the universe, and it has the highest energy density per unit mass. In this regard, the search for new materials capable of storing hydrogen is an urgent task since hydrogen containers are necessary for the safe storage and transportation of hydrogen with a higher specific density compared to the storage of liquefied gas in metal tanks. Solving this problem is no less important than solving the problem of its production.[1]

There are several approaches for hydrogen storage, but although the solid-state storage method is the least developed, it holds great promise as large hydrogen amounts can be stored in a smaller volume compared to other methods.[2] An ideal hydrogen container material should combine a high mass density of storage, suitable thermolysis temperature, reversibility of the hydrogen evolution process, and fast hydrogen adsorption and desorption kinetics, and the use of nanomaterials, in particular, hexagonal boron nitride (h-BN),[3] seems to be a promising strategy.

Bulk h-BN is a layered material with a structure similar to that of graphene: regular hexagons formed by alternating light nitrogen and boron atoms are bonded through the vertices to form a flat two-dimensional material—a monolayer of hexagonal boron nitride (see Fig. 1).[3–5] These layers are connected through van der Waals forces[6] in AA′ packing with a layer spacing of 0.333 nm along the $\vec{c}$ axis (Fig. 1). Thus, when B and N atoms are vertically adjacent to each other in two adjacent layers, the electron-deficient boron atom and the nitrogen atom bearing an additional electron pair can cause a longitudinal redistribution of the electron cloud density, resulting in the so-called "lip–lip" interaction, which further enhances the interlayer forces.[7] The advantages of hexagonal boron nitride are its stability up to 1000 °C and the presence of charge flow due to the difference in the electronegativity of nitrogen and boron atoms, which provides a higher hydrogen binding energy compared to graphene and therefore makes this material a more promising candidate. Moreover in ref. 8, the researchers showed that the advantage of h-BN over graphene can be explained by the presence of a dihydrogen bond ($N\text{–}H^{\delta+}\text{–}{}^{\delta-}H\text{–}B$) and homopolar interactions ($B\text{–}H^{\delta-}\text{–}{}^{\delta-}H\text{–}B$, $N\text{–}H^{\delta+}\text{–}{}^{\delta+}H\text{–}N$).

Various modifications of hexagonal boron nitride show promising characteristics in the field of hydrogen storage.[9–13] For example, pure BN nanotubes were shown to be able to store up to 2.6 wt% of hydrogen and the deformed ones up to 4.2% at 10 MPa.[14] Some estimations indicate that defective BN-based porous materials can store up to 5.1 wt% of hydrogen, and in the case of the additional introduction of lithium atoms, the storage increases up to 7.5 wt%.[15] The maximum theoretically calculated capacity for the BN-based materials (14.77%) was

---

[a] Emanuel Institute of Biochemical Physics RAS, 119334, 4 Kosigin St., Moscow, Russia. E-mail: zipcool@bk.ru
[b] Aramco Innovations LLC, Aramco Research Center, Moscow, Russia
[c] EXPEC ARC, Saudi Aramco, Dhahran, Saudi Arabia
[d] Plekhanov Russian University of Economics, 117997, 36 Stremyanny per., Moscow, Russia

† Electronic supplementary information (ESI) available. See DOI: **https://doi.org/10.1039/d4cp02466d**

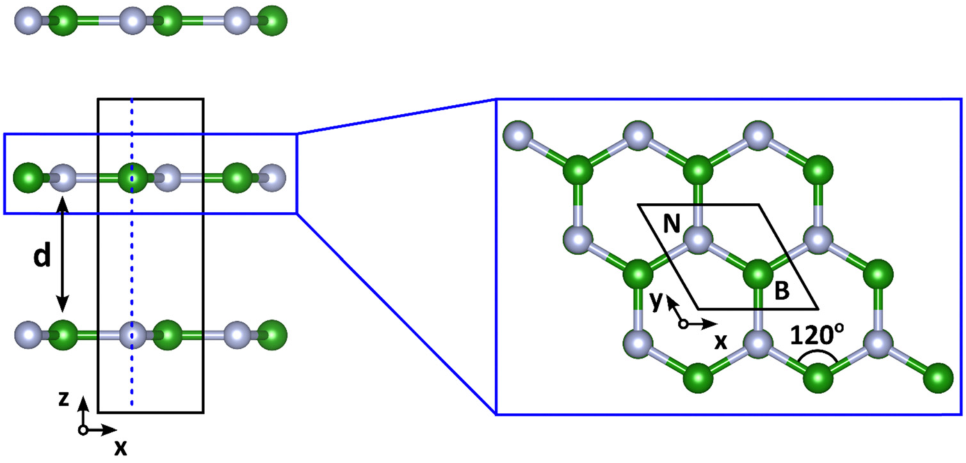

Fig. 1 Atomic structure of a hexagonal boron nitride crystal in AA′ packaging. Green and gray colors indicate boron and nitrogen atoms, respectively. The unit cell is indicated by black lines.

discussed for a C–B–N-based system doped with oxygen and lithium atoms.[16] The experimental modification of h-BN by Ni atoms led to 7.3 wt% of hydrogen storage.[17] In ref. 18 the capacitance characteristics of the hydrogen content in expanded hexagonal boron nitride (eh-BN) were studied using theoretical modeling, and the physical capacity limit for hydrogen stored in an ideal eh-BN system at 243 K and 10 MPa was found to be 2.96 wt%, which corresponds to only 2/5 of the current standard of 7.5 wt% in the automotive industry.[19] In ref. 20 the bilayer h-BN structures in AA′ packing filled with molecular hydrogen were studied theoretically and showed a capacity of up to 4 wt%. These studies indicate the promise of in-depth exploration of h-BN as a hydrogen storage material. However, the full potential of BN utilization for these purposes can be revealed through a deep understanding of the hydrogen interactions in its structure.

Despite a large number of studies in the field of application of boron nitride for hydrogen adsorption, for now, the results reveal a gap related to positive predictions and show inconsistency with each other.[3] Experimental studies require systematic testing of the thermodynamic, kinetic, and cyclic stability of hydrogen absorption and desorption processes with reproducible accuracy meaning that innovative hybrid BN-based structures require the development of a well-defined synthesis procedure. At the same time, all existing monofunctional methods should increase product yield and provide modulation of alloying components or interlayer distance regulation. Therefore it is necessary to combine a practical database with theoretical calculations and elucidate the unique mechanism of hydrogen storage, as well as propose possible modification strategies to subsequently improve the performance of the developed materials.[3]

Besides the h-BN capacity, another important aspect is the mobility of both hydrogen molecules and atoms in the h-BN structure, including diffusion, dissociation, and hydrogen association processes. The possibility of proton transport through one-atom-thick crystals was studied in detail.[21–23] Due to the h-BN layered structure, hydrogen molecule diffusion is possible only in the interlayer space, which limits the number of degrees of freedom of molecule movement through the structure, which, in turn, affects the kinetics of the process. However, if the molecules' movement in a direction perpendicular to the layers is unlikely, then proton diffusion seems to be possible. Since the literature contains rather contradictory data on the value of such diffusion barriers, this indicates that the mechanism has not yet been revealed. Unraveling this mechanism will be of great importance for improving the storage kinetics and the amount of hydrogen stored when h-BN is used as a sorbent.

In ref. 24 the evolution of hydrogen in bubbles coated with a h-BN layer by plasma treatment is discussed. The authors confirmed that multilayer h-BN has a unique porous structure, which, on the one hand, is permeable to atomic hydrogen, but at the same time, on the other hand, is impenetrable to hydrogen molecules. The hydrogen bubbles were shown to persist for a long time without significant changes even after 40 weeks under standard conditions. Considering the bubble structure and the ratio of the stored hydrogen mass to the carrier mass, it is worth recognizing that this approach to hydrogen storage may also be of interest for commercial applications. Experimental evidence of h-BN proton conductivity is presented in ref. 25, where the conductivity of boron nitride sheets was shown to exceed the value for NAFION, indicating the complexity of the hydrogen diffusion mechanism, since the obtained data contradict the previously obtained results of theoretical modeling, according to which the barrier of proton diffusion through a boron nitride sheet is equal to 3 eV[26] and 3.25 eV[27] but at the same time the results in ref. 25 are consistent with the data obtained in ref. 21 where the barrier height was ∼0.7 eV *vs.* 0.3 eV obtained through areal conductivity measurements of the h-BN monolayer.[21] In ref. 28, it was shown that the presence of a second hydrogen atom leads to a decrease in the diffusion barrier value. This fact also finds confirmation in ref. 29 where the proton transfer was studied for the hydrogenated 2D hexagonal layers (exemplified by graphene). Hydrogenation leads to a change in the hybridization of carbon atoms from sp^2 to sp^3, leading to the expansion of lattice cells through which protons penetrate and therefore the proton transfer between layers is facilitated. The hydrogen mobility in h-BN also is important for h-BN performance as a membrane to release hydrogen from a heterogeneous medium[25] or hydrogen compounds.[24] The study of the relationship between hydrogenation and proton transfer in 2D crystals is still ongoing, and further research is needed to fully understand the mechanisms underlying this process. Despite the attempts to generalize data on proton conduction in 2D crystals, a fundamental understanding of the transport mechanisms of proton permeation through atomically thin hexagonal monolayers, including h-BN, is still emerging.[30] Moreover, recent experimental work[24] has generated considerable interest in the detailed study of the proton conductivity characteristics of h-BN.

In the presented work, using density functional theory, a comprehensive theoretical study of the hydrogen sorption and diffusion on h-BN was carried out and the sorption capacity of h-BN structures was investigated.

Computational methods

All quantum-chemical calculations were carried out using density functional theory (DFT)[31,32] realized in the VASP program package.[33–35] The exchange–correlation functional was used in the generalized gradient approximation (GGA) in the revised Perdew–Burke–Ernzerhof (rPBE) parameterization.[36] The method of projector augmented wave was used to describe the ion–electron interaction (PAW)[37] and the cutoff energy of plane waves was equal to 520 eV. Integration in the first Brillouin zone was carried out using theMonkhorst–Pack method.[38] Relaxation of the atomic structure was carried out until the energy difference between the two steps of ion optimization became less than 10^{-4} eV and the energy difference between the two steps of the electronic optimization cycle did not become less than 10^{-5} eV. To avoid interaction between periodic structure images, we used a vacuum region of at least 15 Å in non-periodic directions. Grimm dispersion corrections were applied to describe the van der Waals interaction (DFT-D3 method).[39] The nudged elastic band (NEB)[40] method was used for energy barrier calculations. VESTA[41] and OVITO[42] programs were used to analyze and visualize the atomic structures. The HETEROTOOL program was used for the automatization modeling process.[43]

In the case of H_2 molecule sorption work, we used two definitions of sorption energy: the sorption energy per molecule $\left(E_{\text{ads}}^{\text{H}_2}\right)$ and the sorption energy per h-BN unit $\left(\left\langle E_{\text{ads}}^{\text{H}_2}\right\rangle\right)$ defined as:

$$E_{\text{ads}}^{\text{H}_2} = \frac{E\left[(\text{h-BN})_m + n\text{H}_2\right] - E\left[(\text{h-BN})_m\right] - n\cdot E[\text{H}_2]}{n}$$

$$\left\langle E_{\text{ads}}^{\text{H}_2}\right\rangle = \frac{E_{\text{ads}}^{\text{H}_2}}{m}$$

where $E[(\text{h-BN})_m + n\text{H}_2]$ is the total energy of h-BN with sorbed H_2 molecules, $E[(\text{h-BN})_m]$ and $E[\text{H}_2]$ are the total energies of pristine h-BN and H_2 molecule, respectively, n is the number of sorbed H_2 molecules, and m is the number of h-BN units in the considered supercell. It should be noted that the definition of $E_{\text{ads}}^{\text{H}_2}$ is the same as that used in ref. 44 but the usage of $\left\langle E_{\text{ads}}^{\text{H}_2}\right\rangle$ allows us to additionally take into account the concentration dependence of sorption energy by normalizing by m.

The H atoms' sorption energy was calculated as in ref. 45:

$$E_{\text{ads}}^{\text{H}} = E[\text{h-BN} + n\text{H}] - E[\text{h-BN}] - n\cdot E[\text{H}]$$

where $E[\text{h-BN} + n\text{H}]$ is the total energy of h-BN with sorbed H atoms, $E[\text{h-BN}]$ is the total energy of an isolated h-BN monolayer, $E[\text{H}]$ is the energy of a single H atom calculated from an isolated H_2 molecule, and n is the number of sorbed H atoms.

For the considered systems, the gravimetric storage density (ω) also was calculated as

$$\omega = \left[\frac{nM_{\text{H}_2/\text{H}}}{nM_{\text{H}_2/\text{H}} + M_{\text{h-BN}_{\text{ML}}}}\right] \times 100\%$$

where n is the number of hydrogen molecules or atoms adsorbed on the h-BN monolayer, $M_{\text{H}_2/\text{H}}$ is the molecular weight of the H_2 molecule or H atom, and $M_{\text{h-BN}_{\text{ML}}}$ is the molecular weight of the modeled h-BN monolayer.

Results and discussion

The sorption of molecular hydrogen in pure boron nitride[46] does not show outstanding values of storage suitable for commercial applications (which require at least 6.5 wt%[46]), which may be attributed to the low H_2 sorption energy on the surface of boron nitride sheets. To prove this fact, we calculated the sorption energy of the H_2 molecule on the h-BN monolayer surface for a 5 × 5 × 1 supercell containing one hydrogen molecule (see Fig. S1, ESI†). According to our calculations, the sorption energy of a H_2 molecule on the h-BN monolayer surface $\left\langle E_{\text{ads}}^{\text{H}_2}\right\rangle$ does not significantly depend on the molecule position and orientation relative to the monolayer and is in the range −39.3 meV per H_2 to −55.3 meV per H_2 (see Table S1, ESI†). The obtained results are consistent with the data presented in ref. 47 and 48. The value of sorption energy is comparable to the value of the H_2 molecules bounded in the hydrogen crystal (−48.9 meV per H_2); therefore, the sorption energy corresponds in magnitude to the van der Waals nature. Nonetheless, the sorption energy of single H_2 molecules in the bulk h-BN crystal increases (see Fig. 2) because of the bonding of H_2 molecules with both neighboring h-BN plates. Performed quantum-chemical calculations showed that with an increase in the hydrogen concentration, the sorption energy value of H_2 molecules decreases both in the case of a monolayer (Fig. 2, blue) and bulk (Fig. 2, red) forms of h-BN. For the h-BN monolayer, the calculated sorption energy value becomes positive at a concentration of 5.39 wt% (which correlates well with previously reported results[47,49]), and for the bulk h-BN at a concentration of 12.21 wt% (for more details, see ESI†).

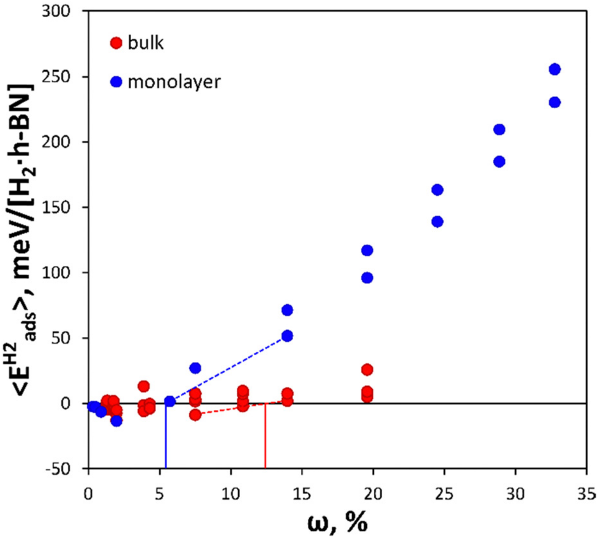

Fig. 2 Dependence of the sorption energy per h-BN unit for a single H_2 molecule on the gravimetric storage density for bulk (red) and monolayered (blue) h-BN.

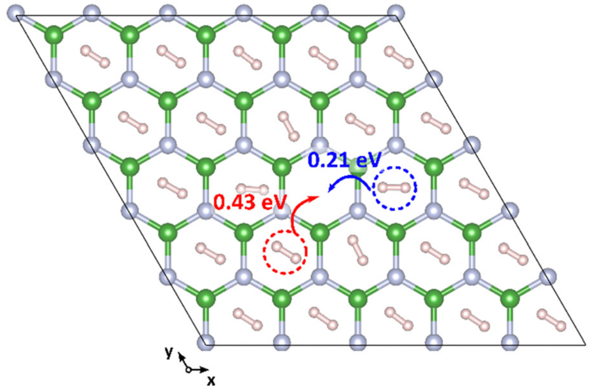

Fig. 3 Diffusion barriers of a single H_2 molecule on the surface of h-BN at a high concentration of H_2 molecules on the surface. The 5 × 5 × 1 supercell of h-BN containing 24 H_2 molecules is indicated by black lines. Green, gray, and pink colors in the inset represent boron, nitrogen, and hydrogen atoms, respectively.

Summing up the above, the low capacity in experimental measurements[46] can be attributed to the initial process of H_2 permeability to h-BN that can limit the use of the entire available area on h-BN sheets. This confirms the fact that BN nanotubes possess much higher hydrogen adsorption capacity than bulk BN powder due to the nanoporous structure and consequently higher specific surface area.[46]

Considering the atomic hydrogen, the calculated sorption energy of a single hydrogen atom on a h-BN monolayer is less than that for molecular hydrogen and is characterized by a positive value equal to 2.50 eV per H (see Table S2, ESI†) with correlates well with previously reported results,[45] while for bulk h-BN the sorption energy is 2.56 eV per H (see Table S3, ESI†). Both high values can be attributed to the covalent-polarized nature of B–N bonds,[50] with high electron localization preventing strong binding of the monolayer to the hydrogen atom. This fact does not allow one to consider the atomic state of hydrogen on h-BN only as an intermediate in the process of diffusion through the structure of boron nitride. But first, it is necessary to understand the behavior of molecular hydrogen on the surface and inside the structure of h-BN.

In addition, the diffusion barrier of H_2 molecules on the h-BN surface is usually considered in terms of the movement of an isolated molecule.[44] According to performed calculations, the diffusion of a single H_2 molecule on the h-BN monolayer is limited by a maximum barrier value of 16.6 meV per H_2 (see Tables S4 and S5, ESI†). Nevertheless, as the hydrogen capacity increases, the diffusion mechanism changes to "vacancy" diffusion and the barrier value increases up to 0.43 eV per H_2 (which corresponds to a 5 × 5 × 1 h-BN supercell covered by 24 molecules with one empty site, see Fig. 3). At a high concentration of hydrogen molecules, the process of diffusion of a single molecule is difficult due to the steric factor and van der Waals interaction of the considered molecule with other hydrogen molecules sorbed on the surface of h-BN; this could explain the change of the diffusion mechanism. Thus, as the H_2 molecule concentration increases, diffusion and desorption processes can become equally probable, which must be taken into account when setting the parameter for multiscale kinetic Monte-Carlo (kMC) simulation,[44] for example.

The modeling of H_2 diffusion in bulk h-BN in parallel to monolayer's surface direction between the centers of neighboring B_3N_3 rings was performed in different supercells of h-BN ($2 \times 2 \times z$, $3 \times 3 \times z$, $4 \times 4 \times z$, $5 \times 5 \times z$, $z = 1, 2, 3$). It was found that the presence of H_2 molecules led to the change in the interlayer distance between neighboring h-BN monolayers clamping the molecule and the value ranges from 3.33 to 5.06 Å (see Fig. 4). The calculated diffusion barrier values correlate with the interlayer distance between BN sheets (see Fig. 4) and are not explicitly dependent on the hydrogen concentration (see Fig. S4, ESI†). By analyzing the obtained values of diffusion barriers one can conclude that for H_2 molecules' easy penetration between the BN sheets, the interlayer width should be enlarged up to 5.06 Å which leads to a decrease in the H_2 diffusion barrier up to 70 meV. At the same time, the interlayer distance equal to 3.33 Å (which is close to that of pristine bulk h-BN) is associated with the 350 meV barrier value hindering the molecule's diffusion from hydrogen-rich areas of h-BN. This fact can explain the long stability (over 40 weeks) of hydrogen bubbles in h-BN observed experimentally[24] and also indicates a greater influence of the interlayer distance on the diffusion barrier than of the hydrogen concentration.[20]

Strong B–N binding in the h-BN network[50] prevents the penetration of molecular hydrogen perpendicular to the sheet direction which can be seen from the analysis of barrier values of H_2 penetration through the h-BN monolayer ranging from 10.00 to 11.73 eV per H_2 (see Table S6, ESI†). High diffusion barrier values make H_2 penetration impossible at a quantifiable time even at different H_2 concentrations (see Fig. S5, ESI†). The significant superiority of the H_2 penetration energy barrier in the 2 × 2 × 1 supercell can be attributed to the limited degrees

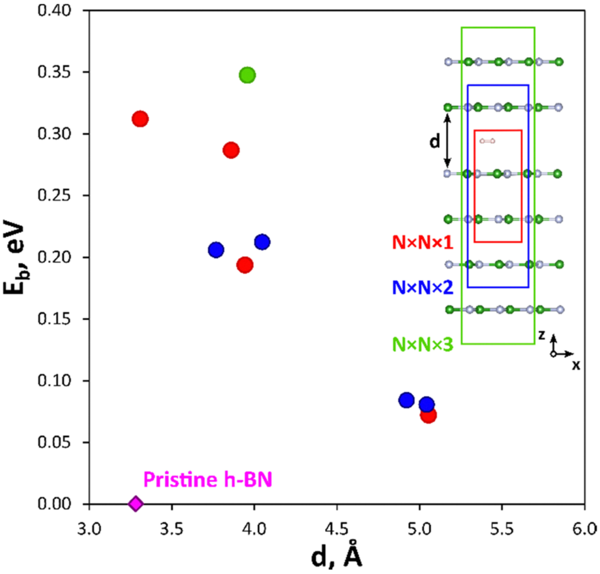

Fig. 4 Dependence of the diffusion barrier of a single H_2 hydrogen molecule in parallel to the monolayer surface direction between the centers of neighboring B_3N_3 rings in the h-BN bulk crystal represented by $N \times N \times z$ supercells (z = 1 (red), 2 (blue), 3 (green)) on the distance between the h-BN layers (d), between which a single H hydrogen molecule is sandwiched. Green, gray, and pink colors in the insert represent boron, nitrogen, and hydrogen atoms, respectively.

of freedom of h-BN deformation in a small cell under periodic conditions in NEB calculations. To summarize, the limited permeability of h-BN by H_2 molecules due to high diffusion barrier values allows us to start considering the diffusion mechanism of atomic hydrogen through the h-BN monolayer.[24,25]

To model single hydrogen atom diffusion through the h-BN monolayer, a 3 × 3 × 1 supercell containing one hydrogen atom located above the center of the B_3N_3 hexagon was considered. The obtained value of the diffusion barrier in the case of physisorbed atom is equal to 3.93 eV and is in good agreement with the data presented in the literature.[26,29] The value for the chemisorbed hydrogen atom is higher and is equal to 4.27 eV (see Fig. 6a). Both values are still high enough to explain the experimentally observed penetration of hydrogen through h-BN sheets.[24] Even stretched (extended) h-BN by 5% (see Fig. S6 and Table S7, ESI†) still demonstrates a relatively high hydrogen atom penetration barrier value of 3.34 eV per H (see Fig. 5).

The key to understanding the experimentally observed atomic hydrogen penetration through h-BN[24] may lie in the effect of the boron nitride sheet passivation by atomic hydrogen. The hydrogenation and gas phase passivation of 2D nitride sheets of group IIIA elements leads to modification of their structural and electronic properties.[51,52] To explore this fact, we considered a 3 × 3 × 1 supercell of h-BN monolayer and studied the sequential diffusion of hydrogen atoms with different passivation of the surface by hydrogen (see Fig. 6).

Firstly, two chemisorbed hydrogen atoms (2H) on neighboring B and N atoms of the BN monolayer were considered (see Fig. 6b). Such a system has two possible ways of single H atom diffusion: (1) through the B_3N_3 hexagon, on which two

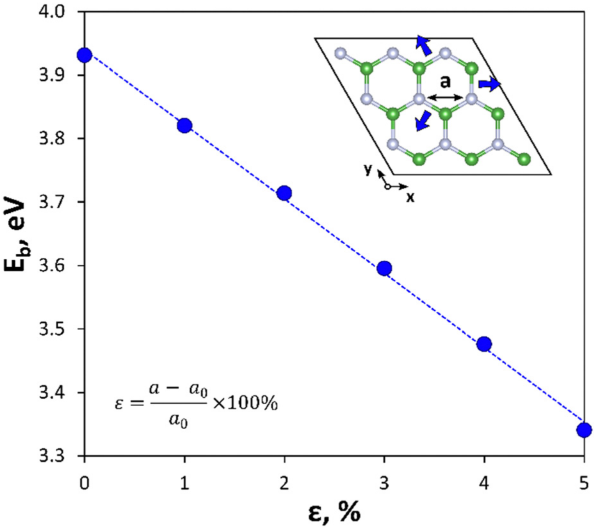

Fig. 5 Dependence of the diffusion barrier value (E_b) of a physisorbed hydrogen atom through the h-BN monolayer on the monolayer stretching value (ε). Inset left: a_0 and a are the cell parameters of the non-deformed and stretched h-BN monolayer. Inset right: Green, gray, and pink colors in the inset represent boron, nitrogen, and hydrogen atoms, respectively.

hydrogen atoms are sorbed, and (2) through the B_3N_3 hexagon, on which one hydrogen atom is sorbed. The diffusion barrier of a single hydrogen atom was found to be less in the case of diffusion way (1), which can be explained by the greater deformation of the B_3N_3 hexagon with two sorbed hydrogen atoms. Both the obtained values of 1.40 eV and 2.97 eV are significantly less than the barrier value for the case of one chemisorbed hydrogen atom meaning that the diffusion of the atomic hydrogen occurs more actively in the presence of several chemisorbed hydrogen atoms on the surface of h-BN, which correlates with the previously reported results.[28] It is also worth noting that the configuration in which hydrogen atoms are chemisorbed on both surfaces of the h-BN monolayer is energetically more advantageous than the sorption on the one h-BN surface.

Configurations (3H, 4H, and 5H) with 3, 4, and 5 hydrogen atoms sorbed on the h-BN surface were also considered (see Fig. 6c, d and e). The lowest barrier value for H penetration was found to be equal to 1.07 eV for 1/3→2/2 transition. But to achieve a 3\1 configuration, it is necessary that at least one hydrogen atom has already penetrated through the surface, and of all the considered the configuration 2\0 has the lowest barrier of 1.41 eV. Based on performed NEB calculations, the following mechanism of hydrogen atom penetration can be proposed: the first hydrogen atom can penetrate with the lowest barrier of 1.41 eV from the 2/0 configuration, and the second atom can diffuse after the sorption of two additional hydrogen atoms leading to the formation of 1/3 configuration to implement the 1/3→2/2 transition with a barrier value of 1.07 eV. Thus, the formation of islands with chemisorbed hydrogen atoms has the greatest effect on lowering the hydrogen atom penetration barrier value. The proposed mechanism can explain the formation of hydrogen bubbles in h-BN *via* plasma treatment[24] and proton penetration through the h-BN

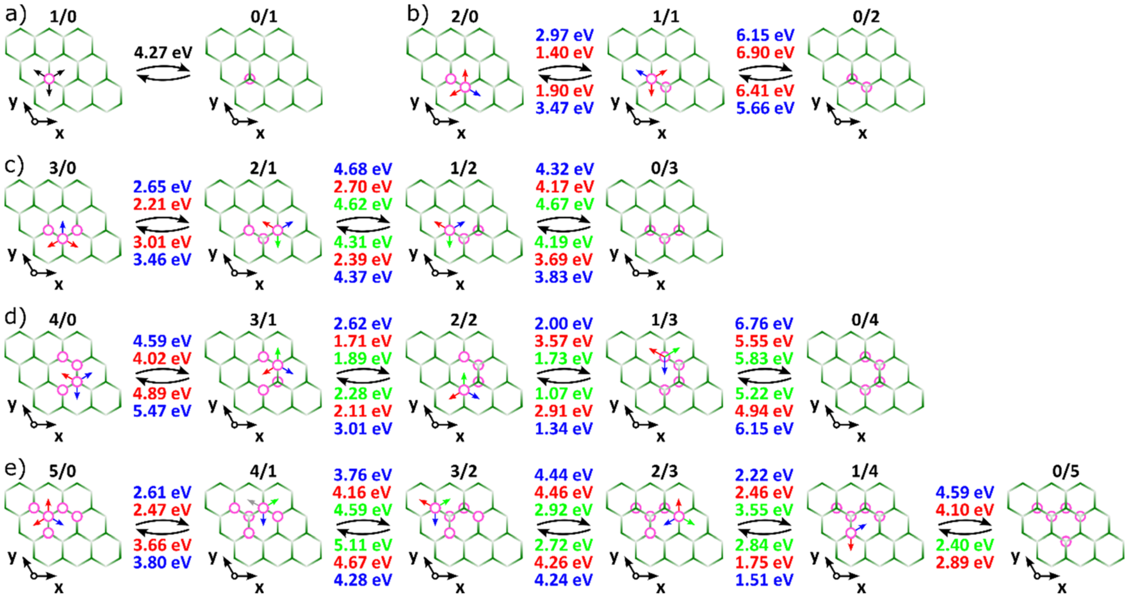

Fig. 6 Considered diffusion pathways for sequential diffusion of individual chemisorbed hydrogen atoms through the h-BN monolayer and the corresponding diffusion barrier values. Green, gray, and pink colors in the inset represent boron, nitrogen, and hydrogen atoms, respectively.

membrane which also was previously associated with charge transfer in solutions.[23,29]

Conclusions

Despite the great potential of hexagonal boron nitride as a versatile material that can both store hydrogen and effectively isolate it from hydrogen-containing molecules under plasma conditions, the exact mechanism of hydrogen penetration through the h-BN sheet is still unclear. We theoretically investigated a potential mechanism by which hydrogen can penetrate through a sheet of h-BN and showed that the h-BN surface passivation results in a decrease in the hydrogen penetration barrier by up to 1.07 eV meaning that this stage may initiate the whole process. We found that bulk h-BN can store molecular hydrogen up to 12.21 wt% while a h-BN monolayer can store up to 5.39 wt%.

Conducted research showed that the preservation of hydrogen within bubbles coated with h-BN shown in a study [*Nat. Commun.*, 2019, **10**, 2815. **https://doi.org/10.1038/s41467-019-10660-9**] can be elucidated by two factors: (1) the elevated barriers of H_2 diffusion between densely packed h-BN layers (350 meV) and (2) the heightened H_2 diffusion barrier under a high concentration (430 meV) which occur through a vacancy mechanism.

The conducted research to understand the mechanisms of hydrogen sorption and diffusion can assist in selecting methods for integrating hydrogen separation and storage technology.

Data availability

The data supporting this article have been included as part of the ESI.†

Conflicts of interest

There are no conflicts to declare.

References

1 F. Zhang, P. Zhao, M. Niu and J. Maddy, *Int. J. Hydrogen Energy*, 2016, **41**, 14535–14552.
2 C. Tarhan and M. A. Çil, *J. Energy Storage*, 2021, **40**, 102676.
3 W. Li, L. Jiang, W. Jiang, Y. Wu, X. Guo, Z. Li, H. Yuan and M. Luo, *J. Mater. Res. Technol.*, 2023, **26**, 2028–2042.
4 D. Gonzalez-Ortiz, C. Salameh, M. Bechelany and P. Miele, *Mater. Today Adv.*, 2020, **8**, 100107.
5 S. Roy, X. Zhang, A. B. Puthirath, A. Meiyazhagan, S. Bhattacharyya, M. M. Rahman, G. Babu, S. Susarla, S. K. Saju, M. K. Tran, L. M. Sassi, M. A. S. R. Saadi, J. Lai, O. Sahin, S. M. Sajadi, B. Dharmarajan, D. Salpekar, N. Chakingal, A. Baburaj, X. Shuai, A. Adumbumkulath, K. A. Miller, J. M. Gayle, A. Ajnsztajn, T. Prasankumar, V. V. J. Harikrishnan, V. Ojha, H. Kannan, A. Z. Khater, Z. Zhu, S. A. Iyengar, P. A. D. S. Autreto, E. F. Oliveira, G. Gao, A. G. Birdwell, M. R. Neupane, T. G. Ivanov, J. Taha-Tijerina, R. M. Yadav, S. Arepalli, R. Vajtai and P. M. Ajayan, *Adv. Mater.*, 2021, **33**, 2101589.
6 A. Pakdel, C. Zhi, Y. Bando and D. Golberg, *Mater. Today*, 2012, **15**, 256–265.
7 Z. Liu, A. Dibaji, D. Li, S. Mateti, J. Liu, F. Yan, C. J. Barrow, Y. Chen, K. Ariga and W. Yang, *Mater. Today*, 2021, **44**, 194–210.
8 Z. Huang and T. Autrey, *Energy Environ. Sci.*, 2012, **5**, 9257–9268.
9 A. Lale, S. Bernard and U. B. Demirci, *ChemPlusChem*, 2018, **83**, 893–903.

10 A. M. Kovalskii, A. M. Manakhov, P. A. Afanasev, Z. I. Popov, A. T. Matveev and A. S. Al-Qasim, *Front. Mater.*, 2024, **11**, 1375977.

11 M. I. Khan, M. U. Amin, S. A. Buzdar, G. Nabi, M. B. Tahir and S. S. Alarfaji, *Int. J. Hydrogen Energy*, 2024, **65**, 727–739.

12 Z. Zhong, X. Gao, L. Huang, H. Wang, Y. Zhao and M. Zhu, *Int. J. Hydrogen Energy*, 2024, **79**, 609–618.

13 A. Kose and M. F. Fellah, *Int. J. Hydrogen Energy*, 2024, **79**, 1086–1099.

14 N. S. Venkataramanan, M. Khazaei, R. Sahara, H. Mizuseki and Y. Kawazoe, *Chem. Phys.*, 2009, **359**, 173–178.

15 H. Zhang, C.-J. Tong, Y. Zhang, Y.-N. Zhang and L.-M. Liu, *J. Mater. Chem. A*, 2015, **3**, 9632–9637.

16 R. Y. Sathe, T. J. Dhilip Kumar and R. Ahuja, *Int. J. Hydrogen Energy*, 2023, **48**, 12767–12795.

17 H. Liang, B. Cao, J. Zhu, X. Shen, M. Zhu, B. Geng, P. Zhang, S. Zhu, F. Yu, R. Zhang, H. Tang, Q. Yuan, J. Li, W. Li and Y. Chen, *Appl. Surf. Sci.*, 2022, **604**, 154118.

18 P. Fu, J. Wang, R. Jia, S. Bibi, R. I. Eglitis and H.-X. Zhang, *Comput. Mater. Sci.*, 2017, **139**, 335–340.

19 Y. J. Colón, D. Fairen-Jimenez, C. E. Wilmer and R. Q. Snurr, *J. Phys. Chem. C*, 2014, **118**, 5383–5389.

20 D. P. Rai, B. Chettri, P. K. Patra and S. Sattar, *ACS Omega*, 2021, **6**, 30362–30370.

21 S. Hu, M. Lozada-Hidalgo, F. C. Wang, A. Mishchenko, F. Schedin, R. R. Nair, E. W. Hill, D. W. Boukhvalov, M. I. Katsnelson, R. A. W. Dryfe, I. V. Grigorieva, H. A. Wu and A. K. Geim, *Nature*, 2014, **516**, 227–230.

22 M. Seel and R. Pandey, *2D Mater.*, 2016, **3**, 025004.

23 L. Shi, A. Xu, G. Chen and T. Zhao, *J. Phys. Chem. Lett.*, 2017, **8**, 4354–4361.

24 L. He, H. Wang, L. Chen, X. Wang, H. Xie, C. Jiang, C. Li, K. Elibol, J. Meyer, K. Watanabe, T. Taniguchi, Z. Wu, W. Wang, Z. Ni, X. Miao, C. Zhang, D. Zhang, H. Wang and X. Xie, *Nat. Commun.*, 2019, **10**, 2815.

25 S. I. Yoon, D.-J. Seo, G. Kim, M. Kim, C.-Y. Jung, Y.-G. Yoon, S. H. Joo, T.-Y. Kim and H. S. Shin, *ACS Nano*, 2018, **12**, 10764–10771.

26 J. M. H. Kroes, A. Fasolino and M. I. Katsnelson, *Phys. Chem. Chem. Phys.*, 2017, **19**, 5813–5817.

27 S. K. Bull, T. A. Champ, S. V. Raj, R. C. O'Brien, C. B. Musgrave and A. W. Weimer, *Appl. Surf. Sci.*, 2021, **565**, 150428.

28 J. M. H. Kroes, A. Fasolino and M. I. Katsnelson, *Phys. Chem. Chem. Phys.*, 2016, **18**, 19359–19367.

29 Y. Feng, J. Chen, W. Fang, E.-G. Wang, A. Michaelides and X.-Z. Li, *J. Phys. Chem. Lett.*, 2017, **8**, 6009–6014.

30 P. R. Kidambi, P. Chaturvedi and N. K. Moehring, *Science*, 2021, **374**, eabd7687.

31 P. Hohenberg and W. Kohn, *Phys. Rev.*, 1964, **136**, B864–B871.

32 W. Kohn and L. J. Sham, *Phys. Rev.*, 1965, **140**, A1133–A1138.

33 G. Kresse and J. Furthmüller, *Phys. Rev. B: Condens. Matter Mater. Phys.*, 1996, **54**, 11169–11186.

34 G. Kresse and J. Furthmüller, *Comput. Mater. Sci.*, 1996, **6**, 15–50.

35 G. Kresse and J. Hafner, *Phys. Rev. B: Condens. Matter Mater. Phys.*, 1994, **49**, 14251–14269.

36 B. Hammer, L. B. Hansen and J. K. Nørskov, *Phys. Rev. B: Condens. Matter Mater. Phys.*, 1999, **59**, 7413–7421.

37 P. E. Blöchl, *Phys. Rev. B: Condens. Matter Mater. Phys.*, 1994, **50**, 17953–17979.

38 H. J. Monkhorst and J. D. Pack, *Phys. Rev. B: Solid State*, 1976, **13**, 5188–5192.

39 S. Grimme, *J. Comput. Chem.*, 2004, **25**, 1463–1473.

40 G. Henkelman, B. P. Uberuaga and H. Jónsson, *J. Chem. Phys.*, 2000, **113**, 9901–9904.

41 K. Momma and F. Izumi, *J. Appl. Crystallogr.*, 2011, **44**, 1272–1276.

42 A. Stukowski, *Modell. Simul. Mater. Sci. Eng.*, 2009, **18**, 015012.

43 D. V. Barilyuk, E. V. Sukhanova, Z. I. Popov, A. A. Korol, A. S. Konopatsky and D. V. Shtansky, *Materials*, 2022, **15**, 8759.

44 S. Ghosh, P. Nath, S. Moshat and D. Sanyal, *Phys. Scr.*, 2024, **99**, 045913.

45 R. Hao, J. Shi, L. Zhu, L. Ji, T. Sun and S. Feng, *Superlattices Microstruct.*, 2017, **111**, 696–703.

46 R. Ma, Y. Bando, H. Zhu, T. Sato, C. Xu and D. Wu, *J. Am. Chem. Soc.*, 2002, **124**, 7672–7673.

47 W. Lei, H. Zhang, Y. Wu, B. Zhang, D. Liu, S. Qin, Z. Liu, L. Liu, Y. Ma and Y. Chen, *Nano Energy*, 2014, **6**, 219–224.

48 J.-X. Kang, K. Harrath and X. Chen, *Theor. Chem. Acc.*, 2021, **140**, 1–6.

49 B. Chettri, P. K. Patra, N. N. Hieu and D. P. Rai, *Surf. Interfaces*, 2021, **24**, 101043.

50 G. Mierzwa, A. J. Gordon and S. Berski, *J. Mol. Model.*, 2020, **26**, 136.

51 E. F. De Almeida, A. Kakanakova-Georgieva and G. K. Gueorguiev, *Materials*, 2024, **17**, 616.

52 R. R. Q. Freitas, G. K. Gueorguiev, F. De Brito Mota, C. M. C. De Castilho, S. Stafström and A. Kakanakova-Georgieva, *Chem. Phys. Lett.*, 2013, **583**, 119–124.